Photosynthesis Research **82:** 59–72, 2004.

Regular paper

Loss of functional Photosystem II reaction centres in zooxanthellae of corals exposed to bleaching conditions: using fluorescence rise kinetics

R. Hill[1], A.W.D. Larkum[2], C. Frankart[1,3], M. Kühl[4] & P.J. Ralph[1,*]
[1]*Institute for Water and Environmental Resource Management and Department of Environmental Sciences, University of Technology, Sydney, Westbourne St Gore Hill, NSW 2065, Australia;* [2]*School of Biological Sciences, University of Sydney, NSW 2006, Australia;* [3]*Laboratoire d'Electrophysiologie des Membranes, Université Paris 7, CASE 7069, 2 place Jussieu, 75251 Paris Cedex 05, France;* [4]*Marine Biological Laboratory, University of Copenhagen, Strandpromenaden 5, 3000 Helsingør, Denmark; *Author for correspondence (e-mail: peter.ralph@uts.edu.au; fax: +61-2-9514-4003)*

Received 12 January 2004; accepted in revised form 29 March 2004

Key words: Chlorophyll-*a* fluorescence, coral bleaching, fast-induction kinetics, OJIP, PAM, PEA, Photosystem II

Abstract

Mass coral bleaching is linked to elevated sea surface temperatures, 1–2 °C above average, during periods of intense light. These conditions induce the expulsion of zooxanthellae from the coral host in response to photosynthetic damage in the algal symbionts. The mechanism that triggers this release has not been clearly established and to further our knowledge of this process, fluorescence rise kinetics have been studied for the first time. Corals that were exposed to elevated temperature (33 °C) and light (280 μmol photons m^{-2} s^{-1}), showed distinct changes in the fast polyphasic induction of chlorophyll-*a* fluorescence, indicating biophysical changes in the photochemical processes. The fluorescence rise over the first 2000 ms was monitored in three species of corals for up to 8 h, with a PEA fluorometer and an imaging-PAM. *Pocillopora damicornis* showed the least impact on photosynthetic apparatus, while *Acropora nobilis* was the most sensitive, with *Cyphastrea serailia* intermediate between the other two species. *A. nobilis* showed a remarkable capacity for recovery from bleaching conditions. For all three species, a steady decline in the slope of the initial rise and the height of the J-transient was observed, indicating the loss of functional Photosystem II (PS II) centres under elevated-temperature conditions. A significant loss of PS II centres was confirmed by a decline in photochemical quenching when exposed to bleaching stress. Non-photochemical quenching was identified as a significant mechanism for dissipating excess energy as heat under the bleaching conditions. Photophosphorylation could explain this decline in PS II activity. State transitions, a component of non-photochemical quenching, was a probable cause of the high non-photochemical quenching during bleaching and this mechanism is associated with the phosphorylation-induced dissociation of the light harvesting complexes from the PS II reaction centres. This reversible process may account for the coral recovery, particularly in *A. nobilis*.

Abbreviations: φ_{Po} – Psi_{Po}; electron transport efficiencies before Q_A; $\Phi_{PS\ II}$ – effective quantum yield; F_m – dark-adapted maximum fluorescence; F'_m – light-adapted maximum fluorescence; F_o – dark-adapted minimum fluorescence; F_t – steady-state fluorescence; LHC – light harvesting complex; OEC – oxygen evolving complex; O–I_1–I_2–P – peak nomenclature along a fast polyphasic fluorescence rise kinetic transient from F_o to F_m (Neubauer and Schreiber 1987); O–J–I–P – peak nomenclature along a fast polyphasic fluorescence rise kinetic transient from F_o to F_m (Strasser and Govindjee 1992); PAM – pulse amplitude modulated; PEA – plant efficiency analyser; PQ – plastoquinone; PS I – Photosystem I; PS II – Photosystem II; Q_A – oxidised primary quinone electron acceptor of PS II; Q_A^- – reduced primary quinone electron acceptor of PS II; Q_B – oxidised secondary quinone electron acceptor of PS II; Q_B^- – reduced secondary quinone electron

acceptor of PS II; qE – energy-dependent quenching; qI – photoinhibitory quenching; qP – photochemical quenching; qT – state transition quenching; RC – reaction centre; ROS – reactive oxygen species

Introduction

Scleractinian corals contain symbiotic dinoflagellates, known as zooxanthellae. Photosynthetic products of these symbionts provide an essential energy source for the coral host, and the coral host supplies zooxanthellae with essential growth factors, respiratory by-products, as well as protection. This mutualistic relationship is an absolute requirement for the coral host and in the absence of zooxanthellae the corals die. The symbiosis is highly sensitive to environmental conditions (Marshall and Baird 2000; Glynn et al. 2001) and anthropogenic impacts (Jones and Hoegh-Guldberg 1999; Ravindran et al. 1999; Bruno et al. 2001). In the last two decades a phenomenon known as mass coral bleaching, has increased globally (Brown et al. 1996; Brown 1997; Woesik 2001). Mass coral bleaching is characterised by the release of the zooxanthellae from the coral host and a reduction in photosynthetic pigment concentration in the zooxanthellae that remain in the coral. While numerous factors have been shown to be involved in various types of coral bleaching, mass coral bleaching, is associated most commonly with elevated temperatures in the light (Glynn 1984; Cook et al. 1990; Hoegh-Guldberg and Salvat 1995; Jones et al. 2000; Fitt et al. 2001; Yentsch et al. 2002). Importantly, the elevated temperatures involved are only 1–2 °C above mean sea surface summer temperatures in the tropics (Hoegh-Gulberg 1999). A clear understanding of the impacts these bleaching temperatures have on the photophysiology of zooxanthellae is therefore an essential step in identifying the mechanisms and processes associated with coral bleaching.

Photokinetic studies of terrestrial plants have shown that PS II is one of the most light and temperature sensitive components of the photosynthetic apparatus. Use of chlorophyll-*a* fluorescence to monitor PS II activity is well documented in coral bleaching research (Iglesias-Prieto 1995; Jones et al. 1998; Fitt et al. 2001; Jones and Hoegh-Guldberg 2001; Ralph et al. 2001). Chlorophyll-*a* fluorescence allows for non-invasive analysis of the photosynthetic apparatus. When a dark-adapted sample is illuminated, it shows a characteristic induction of fluorescence emission, known as the 'Kautsky' curve. The curve has two phases: first there is a rise to a maximum (F_m) over a period of hundreds of ms, followed by a reduction in fluorescence yield over the next seconds or minutes, to a steady-state level (F_t). The rise to F_m has a number of phases, visible on a $\log_{10}$ time scale: first a rise from the origin ($O \cong F_o$) to an intermediate step (J) and then a second slower rise involving a second intermediate (I) to a peak ($P \cong F_m$; Govindjee 1995). High-resolution (μs) sampling of the fluorescence signal enables additional inflexions in the induction curve to be differentiated. The characteristic peaks in the fast induction kinetics have been assigned letters, such that the intermediate steps have been called 'I_1' and 'I_2' by Neubauer and Schreiber (1987) and then 'J' and 'I' by Strasser and Govindjee (1992) and Strasser et al. (1995).

We provide some background to the processes responsible for many of the fast induction kinetics. For more detailed explanations see specific citations listed in text or following reviews (Govindjee 1995; Lazár 2003; Schreiber 2004). Summarising the causal relationships in the O–J–I–P curve it is clear that, overall, the amount of variable fluorescence is proportional to the extent of reduction of Q_A (Dau 1994; Govindjee 1995) although the primary acceptor of activated P680 is phaeophytin. This is because there is a rapid transfer between phaeophytin and Q_A and little charge recombination for the radical pair ($P680^+$/$phaeo^-$) (Lazár 2003; Schreiber, 2004).

The time course for the redox state of Q_A has been modelled (Trissl et al. 1993; Lavergne and Trissl 1995; Stirbet et al. 1998; Lazár 2003) and is the result of linear electron flow from $P680 \Rightarrow Q_A \Rightarrow Q_B \Rightarrow$ plastoquinone chain (PQ) $\Rightarrow$PS I reaction centre (P700), whilst some charge recombination is possible for $P680^+/Q_A^-$. Under the conditions of $P680^+/phaeo^-/Q_A^-$ there is increased energy dissipation from the antenna, in the form of fluorescence. Furthermore, the system is constrained by the two-electron gate at $Q_A \Rightarrow Q_B \Rightarrow$PQ (Figure 1). A two-electron gate means that the system cannot turnover, until Q_B

has been reduced twice. However, in continuous illumination fluorescence induction curves this does not pose a problem. There is also the additional complication that two types of PS II centres have been observed (α and β) which yield different kinetics (Lavergne and Trissl 1995; Lazár 2003). In light of recent models for continuous fluorescence rise kinetics (induction curves) we describe a very brief summary of what has been proposed.

(1) *O–J rise*. This is the fast initial rise and is brought about by displacement of an electron from P680 to Q_A [in a single turnover flash it is $P680^+/Q_A^-$; Lavorel (1959)]. Since $P680^+$ is a quencher, the fluorescence rise cannot occur until $P680^+$ is reduced and this depends on reduction by Y_z, which in turn depends on accumulation of S2 and S3 states and the membrane potential (see Figure 1). However, within the time scale of our experiment, multiple turnovers are involved which means that there must be a flow of electrons from the oxygen evolving complex (OEC). This component can be inhibited by impairment of OEC activity or quenching by $P680^+$. Quenching by $P680^+$ can come about either by deactivation of high energy states (down-regulation of RC II). Charge recombination of $P680^+/Q_A^-$ could also occur but is unlikely. Therefore, the most likely explanation of an inhibition of the O–J rise component is a loss of activity of OEC or a loss of PS II centres, but down-regulation or charge recombination cannot be discounted.

(2) *J-dip*. The dip after J has generally been attributed to a number of processes: (a) the re-oxidation of Q_A^- by Q_B, (b) additional oxidation pressure induced by activation of P700 and the depletion brought about, thereby, of electron transport intermediates between P700 and Q_B, and (c) activation of ATP synthase and conversion of S2 + S3 to S0 + S1 states. Schreiber and Vidaver (1976) argued that the dip is largely attributable to dark pre-reduction of PQ. This has been indicated in corals, where zooxanthellae have been found to employ chlororespiration in darkness (Jones and Hoegh-Guldberg 2001). Alternatively, the dip has been attributed to (c) the quenching of the S2 + S3 states (Schreiber and Neubauer 1987).

(3) *Dip-I rise*. The dip between I and P was labelled by Munday and Govindjee (1969) and is attributed to the further reduction of Q_A as more Q_A and Q_B become reduced. It is also thought to be affected by heterogeneity due to α and β PS II reaction centres (Strasser et al. 1995; Barthélemy et al. 1997). Schreiber and Neubauer (1987) suggest that this section of the curve is influenced by the kinetics of water-splitting enzymes.

(4) *P peak*. This final component is generally ascribed to the filling of the plastoquinone pool (Lavorel and Etienne 1977). If the system has been dark-adapted and no chlororespiration occurs, PQ will be fully oxidised. In the first few seconds of illumination electron flow out of PQ/PQH_2 is minimal and therefore significant reduction of the PQ pool takes place and this reduces electron flow from Q_A/Q_B, causing even greater reduction of Q_A. Thus, Q_A usually becomes fully reduced and results in F_m (maximum fluorescence yield).

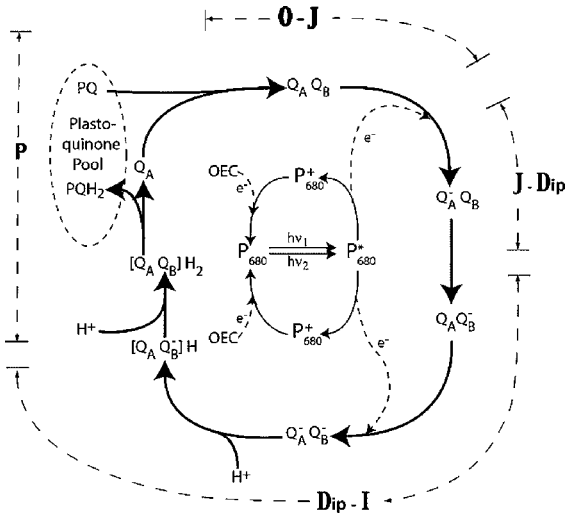

Figure 1. A scheme showing the operation of the two-electron gate mechanism in PS II which couples reduction of Q_A and Q_B to reduction of plastoquinone. This assumes that in the doubly reduced state, $[Q_AQ_B]H_2$, the plastoquinone at the Q_B site is released as a reduced plastoquinol molecule, PQH_2, by diffusion, and is replaced by an oxidised plastoquinone molecule from the plastoquinone pool. Only two stages of the four-stage S-state cycle for the evolution of oxygen and reduction of P680 are shown. On the outer perimeter is shown the approximate timing of the O–J–I–P fluorescence rise components. OEC, oxygen evolving complex.

The analysis of fast induction kinetics under different environmental conditions reveals changes in the physiological state of photosynthetic

organisms, for example as a function of temperature (Guissé et al. 1995; Iglesias-Prieto 1995; Tsimilli-Michael et al. 1999; Pospíšil and Dau 2000), salinity (Barthélemy et al. 1997; Sobrado and Ball 1999; Lu and Vonshak 2002) and light intensity (Koblížek et al. 1999; Srivastava et al. 1999). A detailed analysis of the fast induction curves presented here allows for the discrimination of the relative impact that temperature and actinic light have on the various components of the photosynthetic apparatus. We reasoned that such an analysis would help identify crucial responses of coral photosynthesis to stress factors involved in coral bleaching. This paper shows to our knowledge the first attempt to achieve this goal. Changes in the polyphasic fluorescence rises of corals when exposed to bleaching conditions were investigated.

Materials and methods

Coral specimens

Shallow water corals (< 2 m) were collected from Heron Island lagoon (152°06′ E, 20°29′ S) over the period 26 January to 4 February 2003. Heron Island is located in the Capricorn-Bunker group of islands in the southern Great Barrier Reef of Australia. The three species used were *Pocillopora damicornis* (Linnaeus), *Acropora nobilis* (Dana) and *Cyphastrea serailia* (Forskål). Fast kinetic polyphasic fluorescence rises (Plant Efficiency Analyser [PEA], Hansatech Instruments Ltd, King's Lynn, UK) and concurrent imaging-PAM (Pulse amplitude modulated; Walz, Effeltrich, Germany) data were collected on the three species under bleaching conditions.

All three species were used to investigate impacts on coral photosynthesis by elevated temperatures and the length of exposure to high temperatures. As a control, corals were also maintained at 27 °C under shaded conditions (< 200 μmol photons m^{-2} s^{-1}). As a further control, background fluorescence (PEA and imaging-PAM see below) of the three coral species was measured on specimens, where coral tissue was carefully removed with a Water Pik®. Bleaching treatments were 33 °C for up to 8 h and an irradiance of 280 μmol photons m^{-2} s^{-1} ambient light (halogen lamp 12 V 150 W with UV blocking filter) was applied to each replicate. Four replicates were used and each was placed in a separate dark adaptation chamber (2.8 l) continuously flushed with seawater at experimental temperature (see Hill et al. 2004). Water temperature was maintained using a temperature regulated water bath (Julabo Labortechnik F20-MH, Germany) connected to the chambers. The incubation chambers had a movable shutter, which was closed during dark adaptation. Previous experiments showed that 5 min of dark incubation was sufficient to fully dark adapt the plastoquinone pool and Q_A component (data not shown).

Experimental protocol

As a pre-exposure control response, four replicate corals were exposed for 30 min to 280 μmol photons m^{-2} s^{-1} at 27 °C. Water temperature was then increased to 33 °C (over about an hour) keeping the irradiance constant. Upon reaching 33 °C, a fast induction kinetic measurement of the *in hospite* zooxanthellae was taken and again after 30 min. Hourly measurements from the PEA and imaging-PAM were taken for the next 8 h. Between each fluorescence measurement, the same irradiance was applied to all replicates. Following the 8-h exposure period, the water temperature was lowered to 27 °C, and samples were left in the dark for 10 h. After 10-h dark recovery, samples were exposed for 30 min to 100 μmol photons m^{-2} s^{-1} (low light) and the fast induction kinetics was measured. For the next 10 h, the irradiance was kept at 100 μmol photons m^{-2} s^{-1} and again the fast induction kinetics was determined.

PEA analysis

The polyphasic fluorescence induction kinetics observed in corals under bleaching conditions were analysed using the Plant Efficiency Analyser (PEA) on dark-adapted samples. Illumination was provided by an array of six red LEDs (peak wavelength 650 nm) focussed on an area of 4 mm diameter, resulting in a maximum excitation irradiance of 3200 μmol photons m^{-2} s^{-1}. The fluorescence signal was detected by a PIN-photodiode shielded by a long-pass filter (>720 nm). A saturating flash of 2 s (at 70% of maximum irradiance) was found to provide the optimal polyphasic response. Sub-saturating intensity of the pulse may

impact on the speed of the electron transport in the control. However, in this investigation we are looking for the relative impact of bleaching conditions on photokinetics where these influences will be less significant. The fluorescence signal was recorded every 10 μs for the first 2 ms, every 1 ms for the first 1 s of sampling, and then every 100 ms thereafter up to 2 s. All curves were normalised to the fluorescence yield at 50 μs, F_o, to eliminate any changes linked to a possible reduction in chlorophyll concentration (or zooxanthellae) due to bleaching (Iglesias-Prieto 1995; Tsimilli-Michael et al. 1999; Jones et al. 2000). In addition, the fast kinetic curves were double normalised to F_o and J (1 ms) in order to identify any differences in the curves beyond J.

From the fast induction kinetic data, the initial fluorescence (F_o) was measured at 50 μs, while F_m was measured as the peak fluorescence during the 2-s sampling period. The ratio of F_o/F_m was calculated and this indicates the physiological state of the photosystems. The PS II electron transport efficiency before Q_A (φ_{Po}, linked to maximum quantum yield of excitation energy trapping) was calculated using the following formulae (Lazár 1999):

$$\varphi_{po} = 1 - (F_o/F_m) \quad \text{electron transport efficiency before } Q_A \tag{1}$$

Imaging-PAM analysis

An imaging-PAM system was employed to measure F_t, F'_m, the effective quantum yield of PS II ($[F'_m - F_t]/F'_m$) and photochemical quenching (qP; $(F'_m - F_t)/(F'_m - F_o)$). The imaging-PAM was able to determine the fluorescence signals from the same region where PEA measurements (about 4 mm diameter area) were collected. This provided a confirmation of the photokinetic response.

Statistical analyses

One-way analysis of variance (ANOVA) tests were used to determine if significant differences were present between the different temperature and recovery treatments of the F_o/F_m and F_m parameters, as well as the effective quantum yield data from the imaging-PAM. The assumptions of normality and equal variance were not satisfied for the electron transport efficiency data or the qP data. In these situations, the non-parametric Kruskal–Wallis test was performed. The statistical analyses were performed using the Minitab Statistical Software 13.1 (2000) using a significance level of 0.05 to identify statistically significant differences.

Results

Figures 2a–c shows the fast kinetic induction curves of three coral species, *Pocillopora damicornis*, *Acropora nobilis* and *Cyphastrea serailia* for a series of thermal bleaching treatments. For each species, a selection of characteristic polyphasic curves is shown. In contrast, the background fast kinetic data obtained from coral skeletons, showed no structural features and had an insignificantly low fluorescence reading (data not shown). Figure 2a shows the averaged fast induction curves for *P. damicornis* for four replicates. In the control at 27 °C, a classical O–J–I–P pattern can be observed, indicative of a normal status of various components in the photosynthetic apparatus. The 33 °C 0-h treatment and 1 h treatments had J, I and P peaks higher than the 27 °C control. With longer exposure, these peaks declined with increasing length of exposure to 33 °C. Also F_m decreased with time of exposure. From the control treatment to the 33 °C 4-h treatment, a distinct dip in fluorescence occurred after the J peak, but thereafter was no longer apparent. Figure 3 shows the results where the initial curves of Figure 2 (normalised to F_o) were subsequently normalised to the J peak and the rise to J removed. It can be seen in *P. damicornis* that the curves are all rather similar except that the 10-h recovery treatment which was noticeably higher than the control (Figure 3a). The similarity of all the curves indicates that the major effect of the bleaching treatment was on the initial rise to the J peak.

The polyphasic rise of *P. damicornis* after the 10-h recovery period (viz. after 18 h: 8 h at 33 °C, 9.5 h at 27 °C in darkness, 30 min at 27 °C with 100-μmol photons m^{-2} s^{-1}) was still very low with less inflexions than the control, while the amplitude of F_m was lower than the 8-h 33 °C treatment (Figure 2d). In the 20-h recovery treatment (viz. after 28 h: 8 h at 33 °C, 10 h at 27 °C in darkness, 10 h at 27 °C with 100-μmol photon m^{-2} s^{-1}), the fast induction curve had significantly changed,

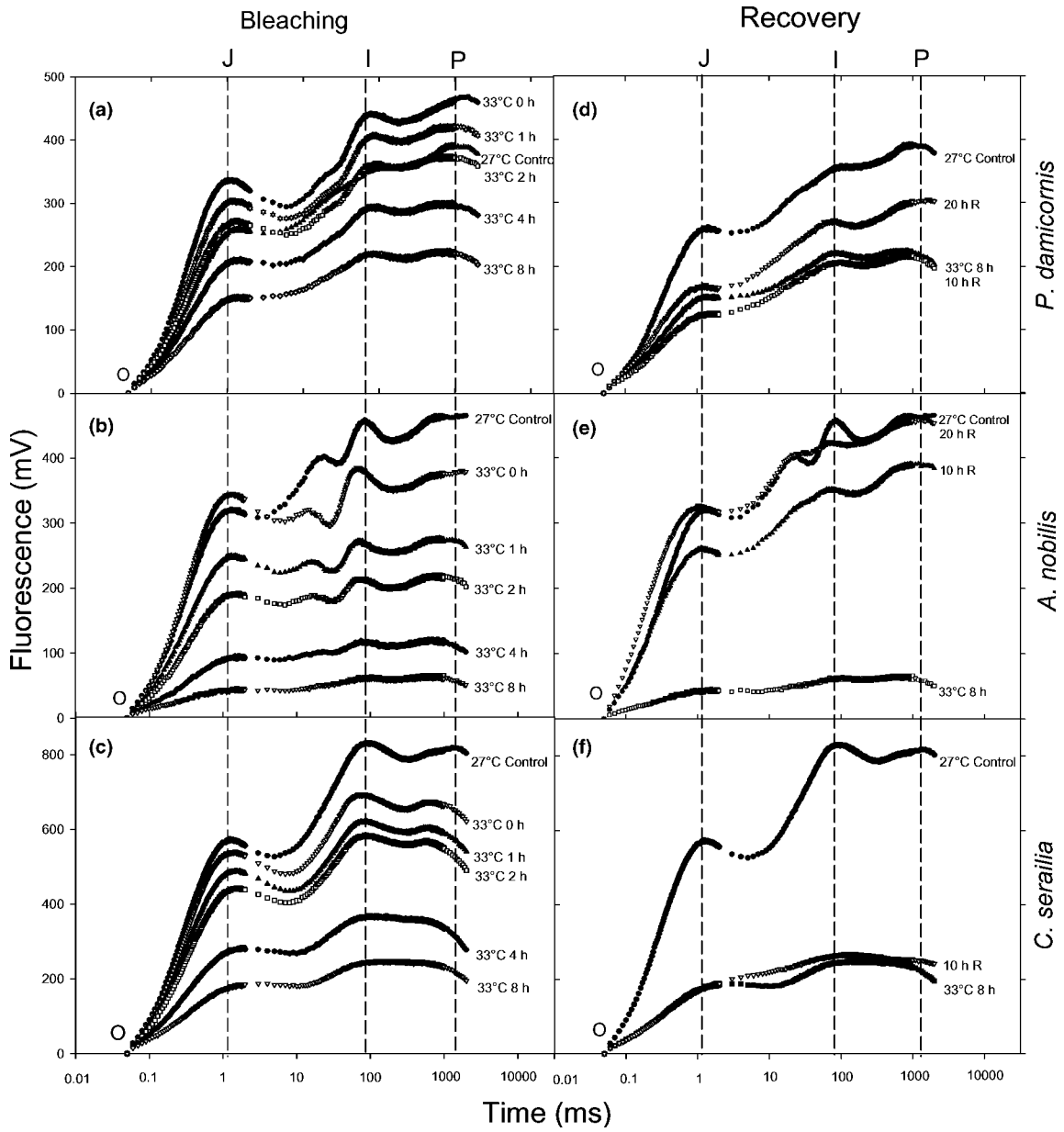

Figure 2. Fast kinetic induction curves of the 33 °C treatments and the recovery treatments. The 27 °C control and 0–8-h 33 °C curves are shown for *Pocillopora damicornis* (a), *Acropora nobilis* (b) and *Cyphastrea serailia* (c). The 10 h R (recovery) and 20 h R (recovery) treatments are also illustrated for *P. damicornis* (d), *A. nobilis* (e) and *C. serailia* (f). Curves are normalised to F_o and are plotted on a $\log_{10}$ time scale. The O, J, I and P peaks are indicated. Average curves are shown ($n = 4$).

including the development of a significant dip between the I and P peaks (Figure 2d). However, all peaks remained lower than those of the 27 °C control treatment.

Figure 2b shows the fast induction curves for *A. nobilis*, which also showed a classical O–J–I–P curve in the control treatment. However, *A. nobilis* showed an unusual new peak between J and I. Unlike *P. damicornis*, the I and P peaks were greater than those of the 33 °C treatments, although the 0-h treatment at 33 °C had a greater J value. The progressive decline in the magnitude of the J, I and P peaks from the control to the 8-h at 33 °C treatment was clearly seen, as was the

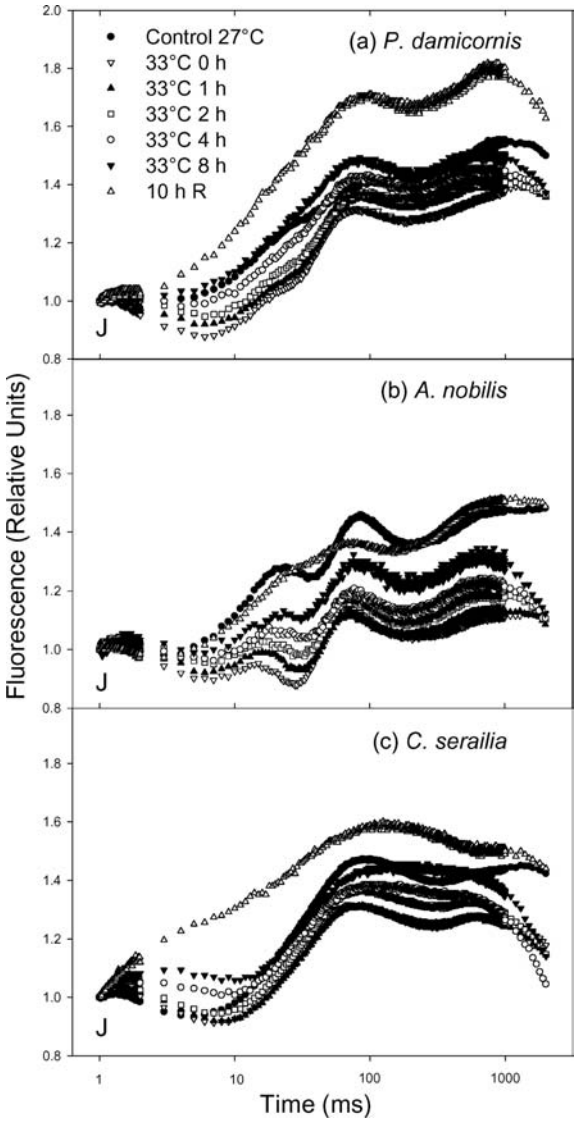

Figure 3. Fast kinetic induction curves double normalised to F_o and J for *Pocillopora damicornis* (a), *Acropora nobilis* (b) and *Cyphastrea serailia* (c). Data from J and onwards is shown. Curves plotted on a $\log_{10}$ time scale. Average curves are shown ($n = 4$).

gradual loss of the inflexion between J and P (Figure 2b). In the 4- and 8-h treatments, no dip was apparent after the J peak. However, after the recovery period the dip re-appeared (Figure 2e). After 4 h at 33 °C, there was no significant difference between the J, I and P fluorescence values. After 8 h at 33 °C, the curve became very smooth. After subtraction of the initial rise and J peak (Figure 3b), the curves are all very similar in amplitude to the control, again indicating a major effect on the initial rise and J peak, with some recovery later, and as in *P. damicornis*, loss of the I peak. Measurements taken after the recovery period (Figure 2e) again showed a greatly increased fluorescence: after 10 h recovery (18-h treatment) the J, I and P peaks had re-appeared. The fast kinetic curve of *A. nobilis* in the 18-h treatment (after 10 h recovery) reached a P peak similar to the 0-h 33 °C treatment (Figure 2e). After 28 h (20 h recovery), the fast kinetic curve increased the amplitude of F_m to be comparable to the control treatment. However, the recovery curves did not show all of the inflexions observed in the control treatment.

The fluorescence induction curves for *C. serailia* (Figure 2c) showed that the 33 °C bleaching treatment caused an effect that was intermediate between that for P. damicornis and *A. nobilis*. There was a strong dip after J for up to 4 h, which did not return in the recovery curves (Figure 2f). Apart from the 10-h recovery treatment, all the curves after normalisation to the J peak were very similar indicating very little effect of the bleaching treatment on later kinetic components of fluorescence rise (Figure 3c). Recovery after 10 h at 27 °C was not apparent. However, the control treatment also showed low responses (Figure 2f). Unfortunately, no 20-h measurement during recovery was possible due to extreme weather conditions, which led to evacuation of the laboratory.

For all 3 species, the F_o/F_m ratio significantly increased (P-values < 0.01) from the control to the 8-h 33 °C treatment (Figure 4). In the recovery treatments, F_o/F_m remained similar to the 8-h 33 °C treatment in *P. damicornis* and *C. serailia*. *A. nobilis*, however, had a F_o/F_m value comparable to the control in both recovery treatments. In contrast, the F_m values significantly declined (P-values < 0.05), but by the 28-h recovery treatment, F_m had returned to a value similar to the control in *P. damicornis* and *A. nobilis* (Figure 4).

The calculated electron transport efficiency before Q_A (φ_{Po}) is shown in Figure 5 for the three species. In *P. damicornis*, φ_{Po} was found to be very similar for all treatments, as no significant differences could be detected ($P > 0.05$). In comparison, *A. nobilis* showed significant decline across the different treatments ($P < 0.001$). The φ_{Po} remained unchanged between the control and 33 °C 0-h treatment. However, following this time φ_{Po} declined rapidly, continuing until the recovery period.

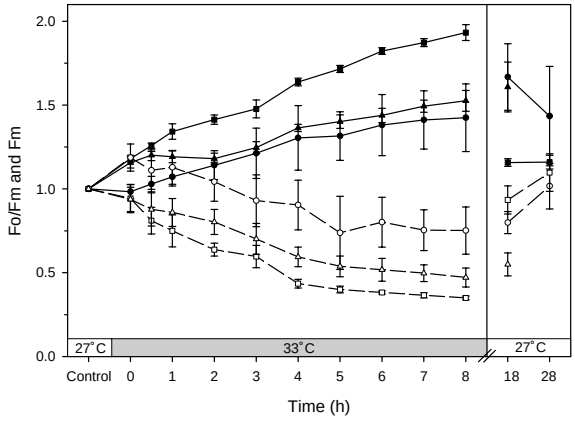

Figure 4. Base fluorescence over maximum fluorescence (F_o/F_m) for *Pocillopora damicornis* (●), *Acropora nobilis* (■) and *Cyphastrea serailia* (▲) (solid lines), and maximum fluorescence (F_m) for *P. damicornis* (○), *A. nobilis* (□) and *C. serailia* (△) (dashed lines). The 27 °C control (normalised to 1), 0–8-h 33 °C treatments and the 18- and 28-h recovery treatments are shown. Data points with error bars indicate averages ± standard error of mean ($n = 4$).

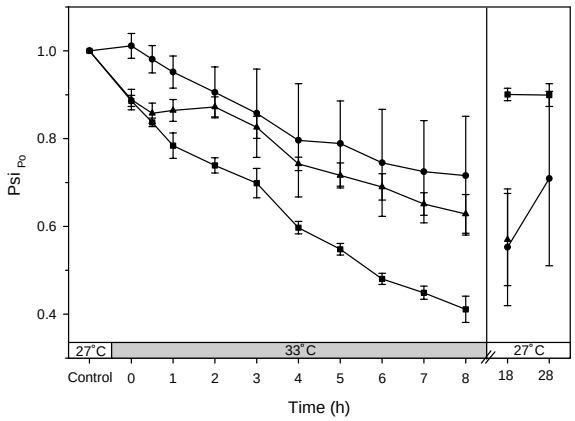

Figure 5. Electron transport efficiency of PS II before Q_A (φ_{Po}; $Psi_{Po} = 1 - (F_o/F_m)$) for *Pocillopora damicornis* (●), *Acropora nobilis* (■) and *Cyphastrea serailia* (▲) (solid lines). The 27 °C control (normalised to 1), 0–8-h 33 °C treatments and the 18- and 28-h recovery treatments are shown. Data points with error bars indicate averages ± standard error of mean ($n = 4$).

After 18 and 28 h, following recovery periods at 27 °C for 10 and 20 h, φ_{Po} had greatly increased and was close to the control value. The φ_{Po} of *C. serailia* declined gradually from the control to the end of the 33 °C treatments and continued to do so in the 10-h recovery treatment for *C. serailia* ($P < 0.05$).

The imaging-PAM was used to confirm the fast induction kinetic responses found by the PEA fluorometer and was employed to measure effective quantum yield ($\Phi_{PS\ II}$; Figure 7) and photochemical quenching (qP; Figure 8). Figure 6 shows representative steady-state chlorophyll fluorescence (F_t) images of *P. damicornis* (a), *A. nobilis* (b) and *C. serailia* (c) captured using the imaging-PAM. The circles indicate the sampling area used to calculate $\Phi_{PS\ II}$ and qP, which is the same sampling area used for the PEA analysis.

The $\Phi_{PS\ II}$ of the three coral species in the control treatment were very similar (Figure 7) and as the length of exposure to bleaching conditions increased the $\Phi_{PS\ II}$ significantly declined ($P < 0.05$). The $\Phi_{PS\ II}$ of *P. damicornis* significantly dropped from the control to the 8-h 33 °C treatment, although the decline was more apparent in the other two species. In *C. serailia*, the $\Phi_{PS\ II}$ declined at a faster rate and even more rapidly in *A. nobilis*. By the 8-h 33 °C treatment, the $\Phi_{PS\ II}$ of *A. nobilis* had reached a value of only 0.06.

The imaging-PAM also determined the photochemical quenching (qP) of these corals (Figure 8). This parameter gave a direct indication of the number of functional PS II RCs, where, a value of 1 indicates all RCs are functional (Büchel and Wilhelm 1993). Under control conditions *A. nobilis* had the greatest amount of qP, whereas *P. damicornis* and *C. serailia* had a slightly lower qP. Upon exposure to the bleaching conditions the qP declined significantly in all species (*P*-values < 0.05), where *A. nobilis* showed the greatest decline. In this species, qP reached zero by the 6-h 33 °C treatment. The other 2 species showed a slower decline in qP, where *C. serailia* had a reading of 0.10 by the 8-h 33 °C treatment. *P. damicornis* showed the smallest decline in qP and by the 8-h 33 °C treatment, it still had a value of 0.58.

Discussion

As shown here, analysis of fast induction curves provides a new and powerful tool for following the molecular events which initiate mass coral bleaching under elevated temperature (33 °C) conditions. In higher plants there are now a number of models which fit closely the fast induction curves (see 'Introduction'). As demonstrated here, fast induction curves of corals under control conditions show a polyphasic O–J–I–P sequence of transients similar to those found with

higher plants, microalgae, and cyanobacteria. These curves are also similar to those found in cultured zooxanthellae (Iglesias-Prieto 1995), although the relative height of the J peak appeared greater with *in hospite* zooxanthellae than with cultured specimens. The three coral species studied here showed several common trends with respect to changes in the magnitude of the fluorescence, presence/absence of peaks and inflexions along the curves under elevated temperature conditions. The J peak occurs as a result of reduction of Q_A to Q_A^- and the transient is known as the photochemical phase (Neubauer and Schreiber 1987; Govindjee 1995). With increasing length of exposure to 33 °C, the fast induction curves all showed a decline in the rate of the initial rise and reduction in the height of the J peak. Guissé et al. (1995) found similar reductions with increasing exposure of potato leaves to high temperatures. This effect, which must be the result of slower reduction of Q_A, has been ascribed to a loss of PS II centres, impairment of electron donation to the primary donor (P680) and an increase in non-photochemical quenching.

Numerous coral bleaching studies have found that PS II efficiency declines in response to elevated light and temperature (Iglesias-Prieto 1995; Warner et al. 1996; Jones et al. 1998). The decline in the activity of PS II could be due to a direct effect of bleaching conditions (33 °C temperatures) on the OEC or, alternatively, to an indirect effect on the number of viable PS II centres, e.g., caused by reactive oxygen species (ROS; Jones et al. 1998). The OEC has been identified as sensitive to bleaching stress (Warner et al. 1996). Fitt and Warner (1995) concluded that elevated light and temperature damaged the oxygen evolving capacity of zooxanthellae from *Montastrea annularis* at temperatures above 30 °C. In our study, analysis of photochemistry before Q_A (φ_{Po}) allowed for a detailed assessment of changes in the capacity for electron transport during this phase of the electron transport chain. φ_{Po} showed a decline during the exposure period and a significant recovery, once temperatures returned to 27 °C. This indicates that the greatest impact was evident before Q_A, which could involve the breakdown or dissociation of the oxygen evolving complex (OEC), or the loss of functional PS II reaction centers. Jones et al. (1998) obtained evidence that the primary effect of bleaching conditions in *P. damicornis* was an effect on CO_2 fixation. They suggested that a backup of electron flow from PS II would lead to greater production of ROS and a resultant impairment of PS II activity. Our study provides evidence for a reduced efficiency of PS II, i.e., the formation of non-functional PS II centres. Firstly, the ratio of F_o/F_m increased during exposure, and decreased again to the control level during the recovery period (Figure 4). As F_m decreased more rapidly than F_o, the ratio F_o/F_m increased. Secondly, the slope of the initial rise and the height of the J peak can be related to the functional capacity of PS II reaction centres (Strasser et al. 1995). With increasing length of exposure to 33 °C, the rate of the initial rise and J declined, indicating inhibition of the PS II reaction centres (Figure 2). Finally, inhibition of PS II activity was evident also in the reduced effective quantum yield shown in the fluorescence images (Figure 7). qP is a direct measure of the number of photochemically active (open) PS II reaction centres, where a value of 1 indicates that all centres are open (Büchel and Wilhelm 1993). The decline seen in Figure 8 indicates a drop in the number of active PS II centres.

Our results could be interpreted to suggest that the major effect of elevated temperature conditions is due to the formation of non-functional PS II reaction centres, rather than an effect on the OEC. Such an effect is more consistent with previous evidence that many released zooxanthellae are in fact quite competent in photosynthesis (Ralph et al. 2001). If the OEC were affected by a rise of temperature from 27 to 33 °C, the effect would be expected to occur much more quickly than the gradual rise over 8 h shown here. Heckathorn et al. (1997) have shown that heat stress in higher plants causes a rapid decline in CO_2 assimilation over 3 h linked to OEC damage.

After the recovery periods, the J responses of the three species were quite different. *P. damicornis* (Figure 2d) and *C. serailia* (Figure 2f) showed only a slight recovery of the J peak, whereas *A. nobilis* (Figure 2e) recovered well and the J peak reached an amplitude equal to the control (27 °C) treatment. This indicates that *A. nobilis* had a high capacity to recover to initial photochemical rates after exposure to stressful, elevated temperature conditions and also indicates that the 10-h recovery period was sufficient for PS II RCs to return to

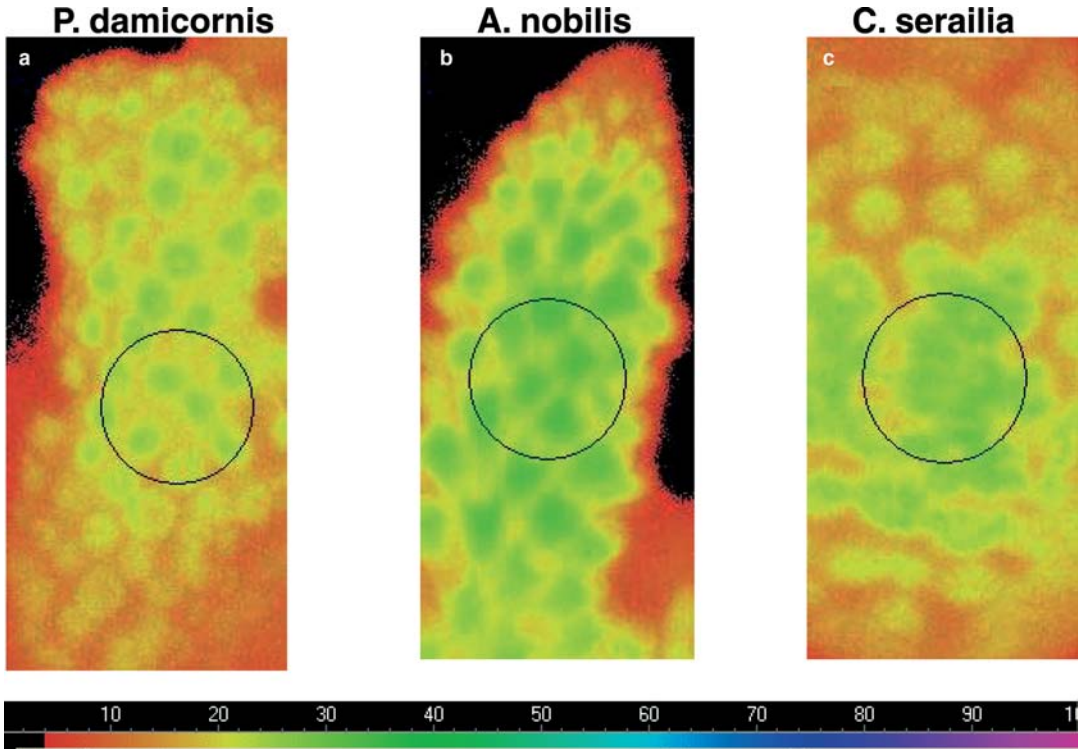

Figure 6. Representative fluorescence (F_t) images of *Pocillopora damicornis* (a), *Acropora nobilis* (b) and *Cyphastrea serailia* (c) from the imaging-PAM. The circles indicate the sample area. The colour gradient scale below indicates the magnitude of the fluorescence signal represented by each colour and circle is 4 mm in diameter.

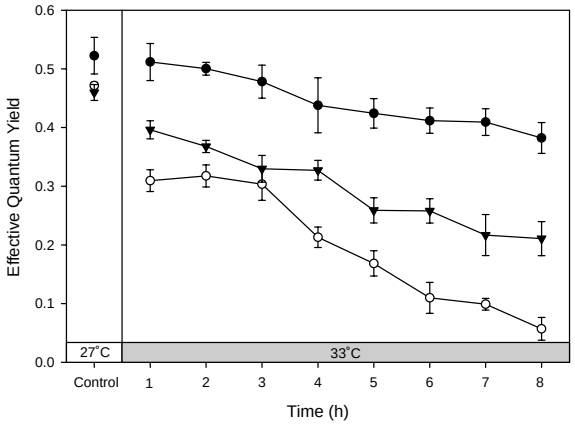

Figure 7. Effective quantum yield ($\Phi_{PS\ II} = (F'_m - F_t)/F'_m$) for *Pocillopora damicornis* (●), *Acropora nobilis* (○) and *Cyphastrea serailia* (▼) for the 27 °C control and 0–8-h 33 °C treatments. Data points with error bars indicate averages ± standard error of mean ($n = 4$).

a functional state. In the other two species investigated here, the capacity for recovery was lower, possibly indicating greater levels of photodamage and/or insufficient time for total recovery. Importantly, the time required to reach J does not vary between each treatment. This result may indicate that the turnover rate of PS II RCs at J does not decline under the temperature treatment, although the number of functional PS II RCs may well have been reduced (see above).

Bleaching has been correlated to a reduction in the PQ pool (Jones and Hoegh-Guldberg 2001), which is implied by the significant drop of the *P* level in almost all treatments exposed to 33 °C. This can be attributed to the blockage of electron donation from the PS II donor side. The plastoquinone (PQ) pool size is therefore represented by the difference in amplitude between the I and P peaks. These I and P steps are thought to be influenced by the presence of fast and slow reducing plastoquinone pool centres, as well as different redox states of the reaction centres responsible for reducing the PQ pool (Strasser et al. 1995; Srivastava et al. 1997). In our control treatments (27 °C), the size of the PQ pool was greatest and gradually decreased in size until conditions became too stressful for any of the PQ

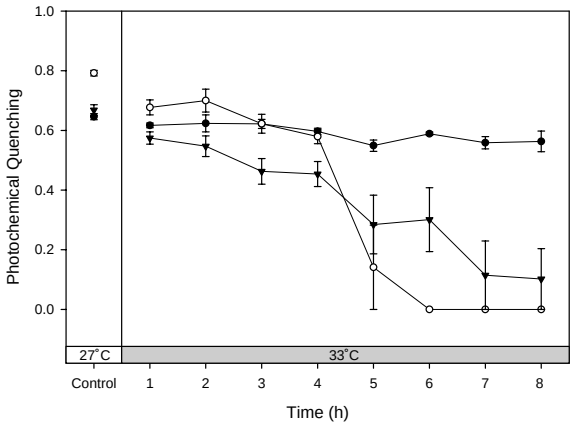

Figure 8. Photochemical quenching ($qP = (F'_m - F_t)/(F'_m - F_o)$) for *Pocillopora damicornis* (●), *Acropora nobilis* (○) and *Cyphastrea serailia* (▼) for the 27 °C control and 0–8-h 33 °C treatments. Data points with error bars indicate averages ± standard error of mean ($n = 4$).

pool to be filled, whereupon the curve became flat (Figures 2a–c). *C. serailia* showed less photoinhibition than the other species, as the PQ pool was still being reduced by the donor side (although very minimally) even by the 8-h 33 °C treatment. Evidence for this was seen in the continued difference between I and P (Figure 2c). The unusual new peak of *A. nobilis* between J and I, may be due to PS I activity in conjunction with PQ. During the dark adaptation period, the plastoquinone pool may become pre-reduced due to low oxygen concentration. Upon illumination PS I may re-oxidise this part of the plastoquinone pool and hence be responsible for this extra peak. Non-photochemical quenching is a process of energy dissipation utilised by photosystems which have absorbed more photons than they can utilise. The relatively steep decline in F_m over time (Figure 4), along with the fact that it decreased faster than F_o, indicates that energy dissipation via non-photochemical quenching was an important mechanism in corals exposed to bleaching conditions. Furthermore, non-photochemical quenching would have influenced the rate of reduction of Q_A, by reducing the amount of energy delivered to the RCs and increasing the amount dissipated as heat. This would have resulted in a slower rate of rise in initial fluorescence and a lower J peak. This indicates a progressive increase in the proportion of energy dissipated as heat and a reduction in energy delivered to the RCs for use in photochemistry. Warner et al. (1996) also found an increase in non-photochemical quenching in corals exposed to increasing light and thermal stress, which supports our findings.

With non-photochemical quenching identified as such an important mechanism in corals exposed to bleaching conditions, it is proposed that it may play an integral role in the formation of non-functional PS II reaction centres. Non-photochemical quenching is comprised of three components; energy-dependent quenching (qE), related to the build-up of a transthylakoid pH-gradient (Demmig-Adams and Winter 1988; Müller et al. 2001), quenching due to state transition (qT), which involves the uncoupling of light-harvesting complexes (LHCs) from PS II reaction centres (Williams and Allen 1987; Haldrup et al. 2001; Müller et al. 2001) and photoinhibitory quenching (qI), which results in long-term photodamage in the photosynthetic apparatus (Krause 1988; Hanelt 1998). The gradual increase in non-photochemical quenching mirrors the decline in functional PS II RCs. The capacity for recovery in each species also shows a close relationship with the amount of non-photochemical quenching. In *A. nobilis* for example, the bleaching conditions reduced the amplitude of the J peak (indicating a loss of functional PS II reaction centres), increased the F_o/F_m and caused a decline in F_m (indicating elevated non-photochemical quenching) (Figure 4). During the recovery treatments, *A. nobilis* returned to conditions very similar to the control with respect to the number of functional PS II reaction centres and the degree of non-photochemical quenching.

These trends indicate that photophosphorylation (involved in state transitions (qT)) may be the component of non-photochemical quenching which plays a role in the formation of non-functional PS II reaction centres. Photophosphorylation involves the dissociation of the LHCs from the PS II reaction centres which allows for excess absorbed energy to be dissipated as heat. This mechanism relaxes over a period of minutes to hours (Demmig-Adams et al. 1989) after which LHCs re-attached to the PS II reaction centres. In these experiments, the recovery treatments showed the reversibility of the impact the bleaching conditions had upon the PS II reaction centres, particularly in *A. nobilis*. Photophosphorylation therefore represents a very powerful mechanism to

limit permanent damage to the photosystems by providing a reversible means of non-functional PS II RC formation. Photophosphorylation would also support other evidence which has demonstrated that expelled zooxanthellae are photochemically competent (Ralph et al. 2001). Further experiments are planned to remove the speculation in this area.

The newly developed imaging pulse amplitude modulated fluorometer (imaging-PAM) was employed in this experiment to confirm and corroborate the data obtained from the PEA under elevated (33 °C) temperatures. While this technique can provide information on many useful parameters (Hill et al. 2004), here changes in effective quantum yield (Figure 7) and qP (Figure 8) were particularly useful in augmenting data from the fluorescence rise experiments. These data showed: (i) a decline in effective quantum yield with elevated temperature, which can be explained by the heat-induced inhibition or down-regulation of the photosynthetic apparatus; and (ii) a reduction in qP, which corroborates a decline in the number of active PS II centres. The area of the coral sampled by the imaging-PAM was similar to the area sampled by the PEA, thus allowing for direct comparisons between data collected by the two instruments. The most sensitive and impacted species was found to be *A. nobilis* (supported by Loya et al. 2001) and the least was *P. damicornis*, with *C. serailia* lying in-between. These data, therefore, not only confirm the information provided by the PEA, but provide extra data on PS II activity and provide information on differences between the polyp and coenosarc tissue (as shown in more detail in Hill et al. 2004).

In summary, we found that the fast fluorescence induction kinetics measurements provided detailed information on the response of corals when exposed to increasing length of exposure to bleaching conditions. This study is the first to use the fast kinetic methodology to investigate *in hospite* coral bleaching. In terms of sensitivity to elevated temperature bleaching conditions, *P. damicornis* was least susceptible and *A. nobilis* was most susceptible with *C. serailia* lying in between. On the other hand, *A. nobilis* showed the ability to recover quickly from bleaching conditions. These results are consistent with another study using the imaging-PAM. The major effect of elevated temperature bleaching conditions was found to be on the initial rise and the height of the J peak. This can be interpreted as an indirect effect on the number of functional PS II centres, possibly as a result of photophosphorylation. The high capacity for recovery in some species may be due to the reversible nature of LHC phosphorylation.

Acknowledgements

We would like to thank the following people: Ulrich Schreiber for his guidance in the operation and interpretation of the Imaging-PAM data, as well as the fast kinetics, Rolf Gademann for field assistance, Neil Ralph for fabrication of the dark-adaptation chambers and Govindjee for editorial comments on an earlier draft. This work was performed with the permission of GBRMPA (permit number G01/623). The Australian Research Council, the University of Technology, Sydney and the University of Sydney provided funding support for AWDL and PJR. MK was supported by the Danish Natural Science Research Council (contract no. 9700549).

References

Barthélemy X, Popovic R and Frank F (1997) Studies on the O–J–I–P transient of chlorophyll fluorescence in relation to Photosystem II assembly and heterogeneity in plastids of greening barley. J Photochem Photobiol B Biol 39: 213–218

Brown BE (1997) Coral bleaching: causes and consequences. Coral Reefs 16: 129–138

Brown BE, Dunne RP and Chansang H (1996) Coral bleaching relative to elevated seawater temperature in the Andaman Sea (Indian Ocean) over the last 50 years. Coral Reefs 15: 151–152

Bruno JF, Siddon CE, Witman JD, Colin PL and Toscano MA (2001) El Niño related coral bleaching in Palau, Western Caroline Islands. Coral Reefs 20: 127–136

Büchel C and Wilhelm C (1993) *In vivo* analysis of slow chlorophyll fluorescence induction kinetics in algae: progress, problems and perspectives. Photochem Photobiol 58: 137–148

Cook CB, Logan A, Ward J, Luckhurst B and Berg CJ (1990) Elevated temperatures and bleaching on a high-latitude coral reef: the Bermuda event. Coral Reefs 9: 45–49

Dau H (1994) Molecular mechanisms and quantitative models of variable Photosystem II fluorescence. Photochem Photobiol 60: 1–23

Demmig-Adams B and Winter K (1988) Characterisation of three components of non-photochemical fluorescence quenching and their response to photoinhibition. Aust J Plant Physiol 15: 163–177

Demmig-Adams B, Winter K, Krüger A and Czygan F (1989) Light response of CO_2 assimilation, dissipation of excess excitation energy, and zeaxanthin content of sun and shade leaves. Plant Physiol 90: 881–886

Fitt WK and Warner ME (1995) Bleaching patterns of four species of Caribbean reef corals. Biol Bull 189: 298–307

Fitt WK, Brown BE, Warner ME and Dunne RP (2001) Coral bleaching: interpretation of thermal tolerance limits and thermal thresholds in tropical corals. Coral Reefs 20: 51–65

Glynn PW (1984) Widespread coral mortality and the 1982–1983 El Niño warming event. Environ Conserv 11: 133–146

Glynn PW, Mate JL, Baker AC and Calderon MO (2001) Coral bleaching and mortality in Panama and Ecuador during the 1997–1998 El Niño-Southern Oscillation event: spatial/temporal patterns and comparisons with the 1982–1983 event. Bull Mar Sci 69: 79–109

Govindjee (1995) Sixty-three years since Kautsky: chlorophyll *a* fluorescence. Aust J Plant Physiol 22: 131–160

Guissé B, Srivastava A and Strasser RJ (1995) The polyphasic rise of the chlorophyll *a* fluorescence (O–K–J–I–P) in heat stressed leaves. Arch Sci (Geneva) 48: 147–160

Haldrup A, Jensen PE, Lunde C and Scheller HV (2001) Balance of power: a view of the mechanism of photosynthetic state transitions. Trends Plant Sci 6: 301–305

Hanelt D (1998) Capability of dynamic photoinhibition in Arctic macroalgae is related to their depth. Mar Biol 13: 361–369

Heckathorn SA, Coleman JS and Hallberg RL (1997) Recovery of net CO_2 assimilation after heat stress is correlated with recovery of oxygen-evolving-complex proteins in *Zea mays* L. Photosynthetica 34: 13–20

Hill R, Schreiber U, Gademann R, Larkum AWD, Kühl M and Ralph PJ (2004) Spatial heterogeneity of photosynthesis and the effect of temperature-induced bleaching conditions in three species of corals. Mar Biol 144: 633–640

Hoegh-Guldberg O (1999) Climate change, coral bleaching and the future of the world's coral reefs. Mar Freshwater Res 50: 839–866

Hoegh-Guldberg O and Salvat B (1995) Periodic mass bleaching and elevated seawater temperatures: bleaching of outer reef slope communities in Moorea, French Polynesia. Mar Ecol Prog Ser 121: 181–190

Iglesias-Prieto R (1995) The effects of elevated temperature on the photosynthetic responses of symbiotic dinoflagellates. In: Mathis P (ed) Photosynthesis: from Light to Biosphere, Vol IV, pp 793–796. Kluwer Academic Publishers, Dordrecht, The Netherlands

Jones RJ and Hoegh-Guldberg O (1999) Effects of cyanide on coral photosynthesis: implications for identifying the cause of coral bleaching and for assessing the environmental effects of cyanide fishing. Mar Ecol Prog Ser 177: 83–91

Jones RJ and Hoegh-Guldberg O (2001) Diurnal changes in the photochemical efficiency of the symbiotic dinoflagellates (Dionphyceae) of corals: photoprotection, photoinactivation and the relationship to coral bleaching. Plant Cell Environ 24: 89–99

Jones RJ, Hoegh-Guldberg O, Larkum AWD and Schreiber U (1998) Temperature-induced bleaching of corals begins with impairment of the CO_2 fixation metabolism in zooxanthellae. Plant Cell Environ 21: 1219–1230

Jones RJ, Ward S, Yang AA and Hoegh-Guldberg O (2000) Changes in quantum efficiency of Photosystem II of symbiotic dinoflagellates of corals after heat stress, and of bleached corals sampled after the 1998 Great Barrier Reef mass bleaching event. Mar Freshwater Res 50: 839–866

Koblížek M, Ciscato M, Komenda J, Kopecký J, Šiffel P and Masojídek J (1999) Photoadaptation in green alga *Spongiochloris* sp. A three fluorometer study. Photosynthetica 37: 307–323

Krause GH (1988) Photoinhibition of photosynthesis. An evaluation of damaging and protective mechanisms. Physiol Plant 74: 566–574

Lavergne J and Trissl HW (1995) Theory of fluorescence induction in Photosystem II: derivation of analytical expressions in a model including exciton-radical-pair equilibrium and restricted energy transfer between photosynthetic units. Biophys J 68: 2474–2492

Lavorel J (1959) Induction of fluorescence in quinone-poisoned *Chlorella* cells. Plant Physiol 34: 204–209

Lavorel J and Etienne AL (1977) *In vivo* chlorophyll fluorescence. Topics Photosynth 2: 203–268

Lazár D (1999) Review: chlorophyll *a* fluorescence induction. Biochim Biophys Acta 1412: 1–28

Lazár D (2003) Chlorophyll *a* fluorescence rise induced by high light illumination of dark-adapted plant tissue studied by means of a model of Photosystem II and considering Photosystem II heterogeneity. J Theor Biol 220: 469–503

Loya Y, Sakai K, Yamazato K, Nakano Y, Sambali H and Van Woesik R (2001) Coral bleaching: the winners and the losers. Ecol Lett 4: 122–131

Lu C and Vonshak A (2002) Effects of salinity stress on Photosystem II function in cyanobacterial *Spirulina platensis* cells. Physiol Plant 114: 405–413

Marshall PA and Baird AH (2000) Bleaching of corals on the Great Barrier Reef: differential susceptibilities among taxa. Coral Reefs 19: 155–163

Müller P, Li X and Niyogi KK (2001) Non-photochemical quenching. A response to excess light energy. Plant Physol 125: 1558–1566

Munday JC and Govindjee (1969) Light-induced changes in the fluorescence yield of chlorophyll *a in vivo* III. The dip and the peak in fluorescence transient of *Chlorella pyrenoidosa*. Biophys J 9: 1–21

Neubauer C and Schreiber U (1987) The polyphasic rise of chlorophyll fluorescence upon onset of strong continuous illumination: I. Saturation characteristics and partial control by the Photosystem II acceptor side. Verl Z Naturf 42: 1246–1254

Pospíšil P and Dau H (2000) Chlorophyll fluorescence transients of Photosystem II membrane particles as a tool for studying photosynthetic oxygen evolution. Photosynth Res 65: 41–52

Ralph PJ, Gademann R and Larkum AWD (2001) Zooxanthellae expelled from bleached corals at 33 °C are photosynthetically competent. Mar Ecol Prog Ser 220: 163–168

Ravindran J, Raghukumar C and Raghukumar S (1999) Disease and stress-induced mortality of corals in Indian reefs and observations on bleaching of corals in the Andamans. Curr Sci 76: 233–237

Schreiber U (2004) Pulse-amplitude-modulation (PAM) fluorometry and saturation pulse method: an overview. In: Papageorgiou GC and Govindjee (eds) Chlorophyll Fluorescence: a Signature of Photosynthesis. Kluwer Academic Publishers, Dordrecht, The Netherlands

Schreiber U and Neubauer C (1987) The polyphasic rise of chlorophyll fluorescence upon onset of strong continuous illumination: II. Partial control by the Photosystem II donor side and possible ways of interpretation. Verl Z Naturf 42: 1255–1264

Schreiber U and Vidaver W (1976) Rapid light-induced changes of energy distribution between Photosystems I and II. FEBS Lett 62: 194–197

Sobrado MA and Ball MC (1999) Light use in relation to carbon gain in the mangrove, *Avicennia marina*, under hypersaline conditions. Aust J Plant Physiol 26: 245–251

Srivastava A, Guissé B, Greppin H and Strasser RJ (1997) Regulation of antenna structure and electron transport in PS II of *Pisum sativum* under elevated temperature probed by the fast polyphasic chlorophyll *a* fluorescence transient: OKJIP. Biochim Biophys Acta 1320: 95–106

Srivastava A, Strasser RJ and Govindjee (1999) Greening of peas: parallel measurements of 77K emission spectra, OJIP chlorophyll *a* fluorescence transients, period four oscillation of the initial fluorescence level, delayed light emission and P700. Photosynthetica 37: 365–392

Stirbet A, Govindjee, Strasser BJ and Strasser RJ (1998) Chlorophyll *a* fluorescence induction in higher plants: modelling and numerical simulation. J Theor Biol 193: 131–151

Strasser RJ and Govindjee (1992) The F_o and the O–J–I–P fluorescence rise in higher plants and algae. In: Argyroudi-Akoyunoglou JH (ed) Regulation of Chloroplasts Biogenesis, pp 423–426. Plenum Press, New York

Strasser RJ, Srivastava A and Govindjee (1995) Polyphasic chlorophyll *a* fluorescence transient in plants and cyanobacteria. Photochem Photobiol 61: 32–42

Trissl HW, Gao Y and Wulf K (1993) Theoretical fluorescence induction curves derived from coupled differential equations describing the primary photochemistry of Photosystem II by an exciton-radical pair equilibrium. Biophys J 64: 974–988

Tsimilli-Michael M, Pêcheux M and Strasser RJ (1999) Light and heat stress adaptation of the symbionts of temperate and coral reef Foraminifers probed *in hospite* by the chlorophyll *a* fluorescence kinetics. Verl Z Naturf 54: 671–680

Warner ME, Fitt WK and Schmidt GW (1996) The effects of elevated temperature on the photosynthetic efficiency of zooxanthellae *in hospite* from four different species of coral reef: a novel approach. Plant Cell Environ 19: 291–299

Williams WP and Allen JF (1987) State 1/state 2 changes in higher plants and algae. Photosynth Res 13: 19–45

Woesik R (2001) Coral bleaching: transcending spatial and temporal scales. Trends Ecol Evol 16: 119–121

Yentsch CS, Yentsch CM, Cullen JJ, Lapointe B, Phinney DA and Yentsch SW (2002) Sunlight and water transparency: cornerstones in coral research. J Exp Mar Biol Ecol 268: 171–183